Steering Angle Control of Rack Steering Vehicle using Antiwindup-PI-Control

Fawzan Khaizuran Faudzi, Addie Irawan*
Robotics, Intelligent Systems & Control Engineering (RISC) Research Group,
Faculty of Electrical & Electronics Engineering Technology, Universiti Malaysia Pahang, Malaysia.
*corresponding author: addieirawan@ump.edu.my

Abstract – *The precision of the steering in a vehicle is one of the issues that need to be tackled for safety and energy efficiencies, especially in the motion at the cornering or turning. The problem is crucial, especially for vehicles with a non-holonomic system such as rack steering vehicles, as it is more prone towards high collisions to the peer walls or off-road incidents due to the inertia factor. Therefore, this study has taken the initiative to propose a steering precision control strategy on Rack Steering Vehicle (RSV) using the proposed antiwindup proportional and integral (API) control. The control objective is to enhance the steering input precision by considering the dynamics of RSV responses that include both vehicle and tire force vectors. Moreover, the API design is emphasized on reducing the friction and other uncertainties in the RSV, which are catered by the antiwindup loop in the control structure. The RSV and the API control are modelled and the the numerical simulation is done with the friction force and aerodynamic force as disturbances. The proposed API was compared with the conventional PID control on the RSV, and the results show that with small fine-tune on the designed API able to compress almost 70% of oscillation in steering angular position response and 3-5% steady-state error from the desired input. The situation gave impact to the vehicle velocity vectors where both horizontal (X-axis) and vertical (Y-axis) velocities are controllable without radical fluctuated speed makes the vehicle with an API controller is 40% slower than with PID in cornering path region. Besides, results also shown that inertia forces are about 25% with PID compare to APID in the cornering region makes this proposed controller able to reduce up to 2kN friction force on average.*

Keywords: *Rack steering vehicle, steering positioning, antiwindup control, dynamics*

Article History
Received 25 February 2020
Received in revised form 15 April 2020
Accepted 16 April 2020

I. Introduction

Rack Steering Vehicle (RSV) has a Non-Holonomic[1] and Non-Skid Steer configuration that open to the oversteered and overdriven as a collateral effect of inertia. Therefore, a dynamic control system is needed. A study for the proposal of the control system has been established where numerous of researches have been done on stable and dynamic path motion especially in cornering, and complex maneuvers to control the mobile robot stability [2], especially on the cornering or turning cases. Inertia plays an essential factor in various dynamic models and control systems, and its control is challenging [3].

Overdriven and oversteer happen due to inertia as friction and other disturbances interfere with the movement of the vehicle. A general explanation on wheeled vehicles, there are two types of wheeled vehicle, the 4-Wheeled Drive which is the typical vehicle that has 4 wheels and Tracked types which is such as tanks or cranes that have multiple wheels and belts around them. For the two-wheeled drive, the are several types of configurations such as Rack Steering and Power Steering, while Track-type wheeled vehicles mostly use differential steering [4]. RSV type is prone to inertial factors according to its non-skid configuration that may contribute to the high chance of collision to walls or off-road incidents from the oversteer and overdrive factor, especially on the cornering tracks.

On the other hand, uncontrollable steering also able to give impact to the internal combustion of the engine, such as discussed by [5], whereby an optimization approach was made on steering control in order to cater the dynamic state of the steering input. It is different from the autonomous vehicle with an electrical power steering system reported by [6] where active disturbance rejection control is applied to estimate the tire self-aligning moment from the calculated steering torque. Zhu *et. al.* discussed that active safety controllers are essential for situations such as emergency braking or braking on the low-friction road [7], thus making the steering and braking control strategy necessary. Enhancement of vehicle handling and stability for safety has become a key research area in designing vehicle systems. A large number of advanced vehicle control systems such as active front steering (AFS), direct yaw moment control (DYC), and torque vectoring (TV) has been developed [8]. The study of integrated control of AFS and DYC has gained much attention from many researchers, such as Fuzzy logic control [9], sliding mode control [10], control allocation method [11], optimal control [12], the model predictive control [12, 13], reconfigurable control [14] and etc.

The objective of the project is to propose a new controller for the steering positioning in RSV in order to reduce the friction and disturbance to avoid inertia factor, especially in cornering path. In this study, RSV numerical model is constructed for simulation and analysis through the dynamic elements of the RSV which includes the velocity, force, and energy.

II. Overview of Rack Steering Vehicle Dynamic Model

In order to determine the inertia of the RSV, analytical calculations using the expression kinetic energy based on the theory of kinematics and dynamics are used. According to the dynamics reference frame as shown in Fig.1 and regarding Newton's law, the equilibrium of forces and momentum of the RSV can be derived as expressed from (1) to (3) [15].

$$\begin{aligned} m\ddot{x} &= (f_{X1}+f_{X2})\cos(\delta_r)+f_{X3} \\ &\quad + f_{X4}-(f_{Y1}+f_{Y2})\sin(\delta_r)+m\dot{\theta}\dot{y} \end{aligned} \tag{1}$$

$$\begin{aligned} m\ddot{y} &= (f_{Y3}+f_{Y4})+(f_{X1}+f_{X2})\sin(\delta_r) \\ &\quad +(f_{Y1}+f_{Y2})\cos(\delta_r)-m\dot{\theta}\dot{x} \end{aligned} \tag{2}$$

$$\begin{aligned} &I_\theta\ddot{\theta} = L_1(f_{X1}+f_{X2})\sin(\delta_r)+L_1(f_{Y1}+f_{Y2})\cos(\delta_r) \\ &-L_2(f_{Y3}+f_{Y4})+\frac{I_\theta}{2}(f_{X2}-f_{X1})\cos(\delta_r) \\ &+\frac{I_\theta}{2}(f_{X4}-f_{X3})+\frac{I_\theta}{2}(f_{Y1}-f_{X2})\sin(\delta_r) \end{aligned} \tag{3}$$

where δ_r is the front-wheel angle, f_{xn} is the longitudinal tire force developed due to road slope of the motion where n=1…4 and f_{yn} is the lateral tire force developed for the same condition with m is the mass of the vehicle. On the other hand, L_1 and L_2 are the dimensions of vehicle squares with the center of gravity (CoG) of the vehicle body, I_θ is the moment inertia for both longitudinal Vy and lateral velocities of the vehicle Vx respectively with is the rotational angle of the vehicle at CoG.

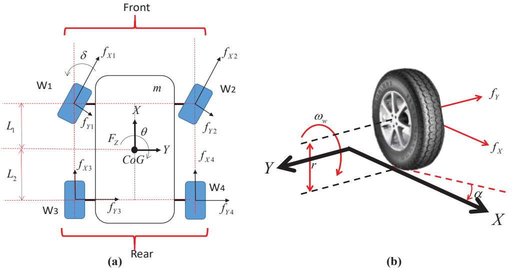

Fig. 1. RSV wheel dynamics motion frame; (a) Vehicle dynamic motion and frames, (b) Wheel rotation friction force[15]

Two types of resistance modeled for RSV, which are drag resistance between the RSV and the wind named as aerodynamics force f_{aero}, and resistance of vehicle's tire itself named as a rolling resistance f_R as expressed in (4) and (5) respectively[15].

$$f_{aero} = \frac{1}{2}\rho C_d A_f (V_X + V_{wind})^2 \tag{4}$$

$$f_R = c(f_{zf}+f_{zr}) \tag{5}$$

III. Antiwindup PI control design

For the goal of enhancing the precision of steering motion and maintaining the literal stability of the RSV, forces vector on the vehicle (F_X, F_Y), as well as force vector on tire (f_X, f_Y), must be well controlled. Therefore, the relation between the steering input and those acting forces need to be identified. From (2), the mathematical expression for the steering angular feedback δ_0 of the RSV is expressed in equation (6) with the relation of vehicle mass m, translation of position for the vehicle (x,y), the angular position of vehicle θ, the angular velocity of vehicle $\dot{\theta}$ and both force vectors on x-axis vehicle and tire represented by F_X and f_X respectively. After a long calculation and derivation, the annotation of C, P, Q, R, S, T, U, and Z are defined from (7) to (13) respectively, with optimum constant value γ=5.09. Here, only Vx is considered since the Vy will duplicate the same effect for the whole vehicle. The objective of the control is to provide stable control of $u(t)$ with reference input δ_r.

$$\delta_o = \frac{C}{(8(-U+P+Q-T+R+S)-T)-\gamma\pi} \tag{6}$$

$$C = 2\left(\tan^{-1}\left(\frac{1}{2}\frac{\left(\sqrt{-8Z^2-4(-P+Q+T+R+S)\cdot(U+P-Q+T+R+S)}+Z\right)}{(U+P-Q+T+R+S)}\right)\right) \tag{7}$$

$$P = \left(m\dot{\theta}\dot{y}\right)t \tag{8}$$

$$Q = m\dot{x} \tag{9}$$

$$R = [mg\sin(\theta)]t \tag{10}$$

$$S = (f_R)t \tag{11}$$

$$T = (f_{X3} + f_{X4})t \quad (12)$$

$$U = (F_{X1} + F_{X2})t \quad (13)$$

The steady-state error for the steering e can be expressed as in (14) as follows;

$$e = \delta_r - \delta_0 \quad (14)$$

where e as input to the proposed Antiwindup Proportional-Integrated (API) controller as shown in Fig.2, which $u(t)$ is back calculated and sum of $e(t)$ with the different order as in (13) as follows,

$$u(t) = K_I \int e(t) + \left[K_P e(t) + u(t)K_w + K_T(t+T)\right]K_T(t) \quad (13)$$

where $K_T = T^{-1}$ which $T = 1ms$ of the processing unit sampling time, K_I is an integral gain and K_w is a back signal control input gain. All these gain tunings will be fine-tuned during the simulation session. This controller is expected to eliminate the overshoot and oscillation in steering motion that contributes to the overdrive. The $u(t)$ to be recalculated to a new value that produces an output when the system reaches to its saturation limit [16, 17].

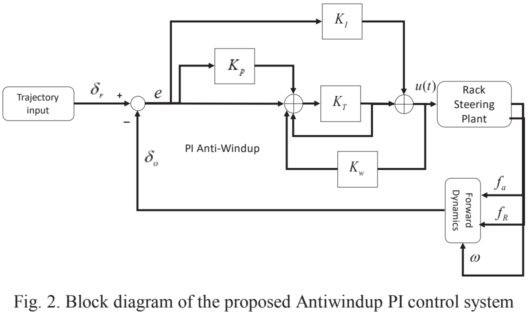

Fig. 2. Block diagram of the proposed Antiwindup PI control system for RSV

TABLE I
PARAMETERS OF RSV MODEL

Parameters	Value
m	1300kg
C_σ	20000
C_α	80000
L_f	1.180
L_r	1.770
L_ω	1.880
gravity	9.81

The parameters of the RSV model is listed in Table I [15]. It consists of gravity, mass m, longitudinal stiffness $C\sigma$, cornering stiffness $C\alpha$, a distance of rear axle from CoG L_f, a distance of front axle from CoG L_r and the distance between the left and right wheels track length L_ω. The block configuration hierarchy is a top-down configuration.

IV. Simulation and Results

The RSV model with the proposed API control was modeled and simulated to verify the performance of the vehicle with the external disturbances, including aerodynamics drag force. The sharp cornering trajectory input was designed as shown in x-y axis plot in Fig. 3, where the vehicle will be having three-point of sharp corners at about (9m, 0.025m), (9.8m, 0.13m) and (11m,-0.05m). These points are the focus area in the analysis and discussions.

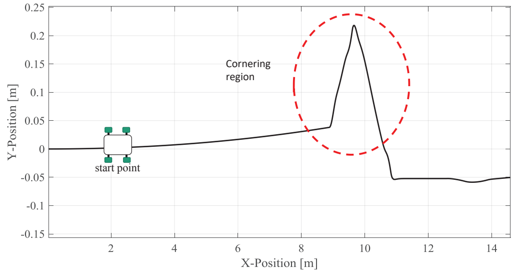

Fig. 3. Trajectory input for RSV in terms of X-Y Cartesian of motion

The proposed API control is compared with the conventional PID controller for the analysis and verification. The aerodynamics force friction is generated and given randomly in the range of 0 to 900N, as shown in Fig. 4. The fine-tuned value for both PID and the proposed API is shown in Table II.

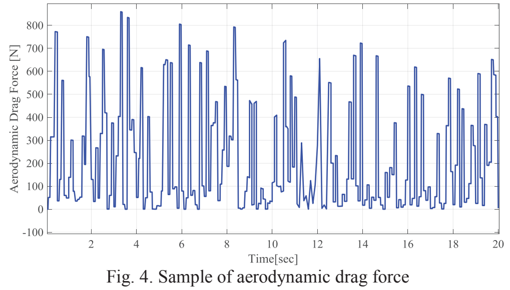

Fig. 4. Sample of aerodynamic drag force

As shown in Fig. 5, the steering input with the PID controller unable to correct much the steady-state error and major on the cornering region between 8 to 12 secs at about 3-5% from the desired input reference. Therefore, this performance resulting in a substantially different in-vehicle axial velocities, as shown in both Fig. 6 and 7.

TABLE II
FINE-TUNED VALUES FOR THE DESIGN PARAMETERS OF THE PID AND APID

Controller	Parameter	Value
PID	K_P	64.0012
	K_I	14.7691
	K_D	0.1
APID	K_P	50.33
	K_I	8.73
	K_W	3.2
	K_T	1000

As shown in Fig. 6, the velocity on X-axis *Vx* with a disturbance comes with the effect. The *Vx* shown is far lower when API is applied compared to the PID, making the vehicle heading a bit slower in the overall vehicle point of view although a bit fluctuated speed in a cornering region that considered as minor around 2 m/s. The results also show that API able to minimize the oscillation on the speed at almost 70% compared to the PID performances. The situation is clearly shown in the cornering region between 8 to 11 secs in Fig. 7. Concerning the sharp corner period as shown in Fig. 5, the RSV is controllable with API, with 40% slower without oscillations compared to PID at the first cornering point and forwards. Table III shows the summary of both controller performances in terms of precision of steering angle control, and Table IV shows the overall performance of the vehicle between controllers.

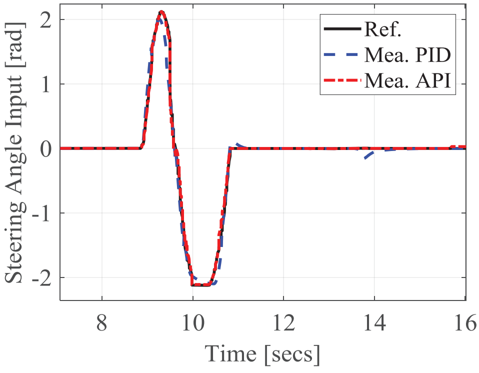

Fig. 5. Steering input performances, with PID versus with API control

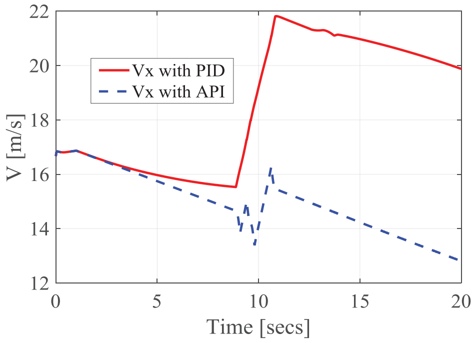

Fig. 6. Velocity on X-axis performances; with PID versus with API control

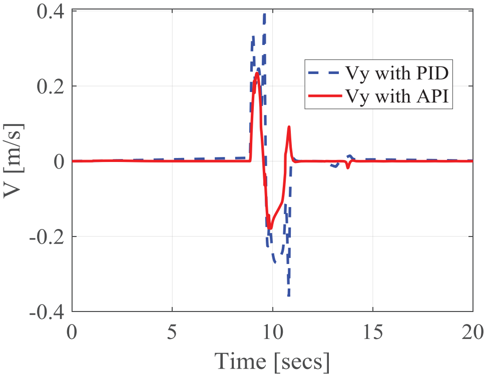

Fig. 7. Velocity on Y-axis performances; with PID versus with API control

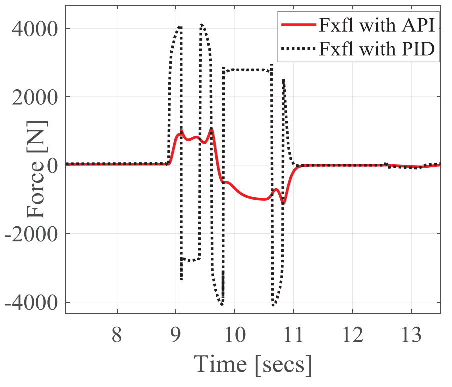

Fig. 8. Inertia Forces at X-axis performances; with PID versus with API control

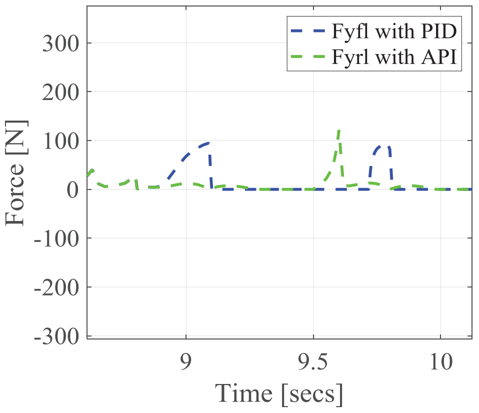

Fig. 9. Inertia Forces at Y-axis performances; with PID versus with API control

TABLE III
SUMMARY OF STEERING ANGLE TRACKING ERROR PERFORMANCES BETWEEN PID AND APID

Par / Contr.	Rise Time	Overshoot	Phase Margin	Settling Time
PID	3.12ms	0.02%	0.81 rad/s	4.09ms
APID	2.07 ms	0%	1.75 rad/s	3.09ms

TABLE IV
SUMMARY OF VEHICLE PERFORMANCES BETWEEN PID AND APID IN CORNERING REGION

Par / Contr.	Average Speed	Average force friction	Average Inertia forces
PID	0.3ms	3kN	80N
APID	0.2 ms	1kN	20N

V. Conclusion

The proposed API was simulated and verified. The results show that the proposed API able to control the steering input tracking error and affects the performance of the overall vehicle by reducing the velocities. The performances are clearly shown in the cornering region, whereby the vehicle takes on three different sharp cornerings as trajectory input. The cause is more prone to inertial force factor that affects the steering motion output corresponding to the overall dynamics of the RSV. The phenomena can be seen in the inertial force performance on both vehicle axes where it is reduced by API with low frictions during the cornering region compared to the RSV with the PID controller.

Acknowledgments

This research and development are supported by the Ministry Of Higher Education Malaysia under the Fundamental Research Grant Scheme (FRGS) (Grant No. FRGS/1/2016/TK04/UMP/02/9) and Universiti Malaysia Pahang (UMP) Research Grant (RDU140351).

References

[1] W. Hashimoto, Y. Yamashita, R. Nonaka, and K. Kobayashi, "Asymptotic Stabilization of Nonholonomic Four-Wheeled Vehicle with Steering Limitation based on Lyapunov Function Approach," *IFAC-PapersOnLine,* vol. 49, pp. 235-240, 2016.

[2] V. Sharma, S. Rathore, N. Sharma, A. Bansal, and G. Saxena, "Implementation of Rack and Pinion Steering System in QUAD Bike," 2018.

[3] J.-S. Zhao, Z.-J. Liu, and J. Dai, "Design of an Ackermann Type Steering Mechanism," *Journal of Mechanical Engineering Science,* vol. 227, 2013.

[4] R. Siegwart, I. R. Nourbakhsh, and D. Scaramuzza, *Introduction to autonomous mobile robots*: MIT press, 2011.

[5] C.-H. Wu, "Optimization of steering control to improve the energy consumption of internal combustion engine vehicles," *Heliyon,* vol. 5, p. e03056, 2019.

[6] L. Xiong, Y. Jiang, and Z. Fu, "Steering Angle Control of Autonomous Vehicles Based on Active Disturbance Rejection Control," *IFAC-PapersOnLine,* vol. 51, pp. 796-800, 2018.

[7] J. Zhu, Z. Wang, L. Zhang, and D. G. Dorrell, "Braking/steering coordination control for in-wheel motor drive electric vehicles based on nonlinear model predictive control," *Mechanism and Machine Theory,* vol. 142, p. 103586, 2019.

[8] H. Mirzaeinejad, M. Mirzaei, and S. Rafatnia, "A novel technique for optimal integration of active steering and differential braking with estimation to improve vehicle directional stability," *ISA Transactions,* vol. 80, pp. 513-527, 2018.

[9] X. Ma, P. K. Wong, J. Zhao, and Z. Xie, "Cornering stability control for vehicles with active front steering system using T-S fuzzy based sliding mode control strategy," *Mechanical Systems and Signal Processing,* vol. 125, pp. 347-364, 2019.

[10] S.-B. Lu, Y.-N. Li, S.-B. Choi, L. Zheng, and M.-S. Seong, "Integrated control on MR vehicle suspension system associated with braking and steering control," *Vehicle System Dynamics,* vol. 49, pp. 361-380, 2011.

[11] O. Temiz, M. Cakmakci, and Y. Yildiz, "Adaptive Control Allocation with Communication Delay for In-Wheel Propulsion Electric Vehicles," *IFAC-PapersOnLine,* vol. 52, pp. 157-162, 2019.

[12] B. Li, H. Du, W. Li, and Y. Zhang, "Side-slip angle estimation based lateral dynamics control for omni-directional vehicles with optimal steering angle and traction/brake torque distribution," *Mechatronics,* vol. 30, pp. 348-362, 2015.

[13] S. D. Cairano, H. E. Tseng, D. Bernardini, and A. Bemporad, "Vehicle Yaw Stability Control by Coordinated Active Front Steering and Differential Braking in the Tire Sideslip Angles Domain," *IEEE Transactions on Control Systems Technology,* vol. 21, pp. 1236-1248, 2013.

[14] B. Németh, P. Gáspár, D. Fenyes, and J. Bokor, "Reconfigurable Control Design of Steering and Torque Vectoring Based on Reachability Set Analysis**The research was supported by the National Research, Development and Innovation Fund through the project "SEPPAC: Safety and Economic Platform for Partially Automated Commercial vehicles" (VKSZ 14-1-2015-0125). This paper was partially supported by the János Bolyai Research Scholarship of the Hungarian Academy of Sciences," *IFAC-PapersOnLine,* vol. 50, pp. 3702-3707, 2017.

[15] N. M. Adam, A. Irawan, and F. K. Faudzi, "Impedance control on rack steering vehicle for inertia shaping on cornering track," *International Journal of Dynamics and Control,* vol. 7, pp. 1434-1442, 2019.

[16] H. Markaroglu, M. Guzelkaya, I. Eksin, and E. Yesil, "Tracking Time Adjustment In Back Calculation Anti-Windup Scheme " presented at the 20TH EUROPEAN Conference on Modelling and Simulation ECMS 2006 Bonn, Germany, 2006.

[17] W. M. N. W. Lezaini, A. Irawan, and S. N. S. Ali, "Forkloader Position Control for A Mini Heavy Loaded Vehicle using Fuzzy Logic-Antiwindup Control," *TELKOMNIKA (Telecommunication Computing Electronics and Control),* vol. 15, pp. 739-745, 2017.